N,*N*-Di(4-halophenyl)nitrenium Ions: Nucleophilic Trapping, Aromatic Substitution, and Hydrogen Atom Transfer

Selina I. Thomas and Daniel E. Falvey*

Department of Chemistry and Biochemistry, University of Maryland, College Park, Maryland 20742

falvey@umd.edu

Received December 15, 2006

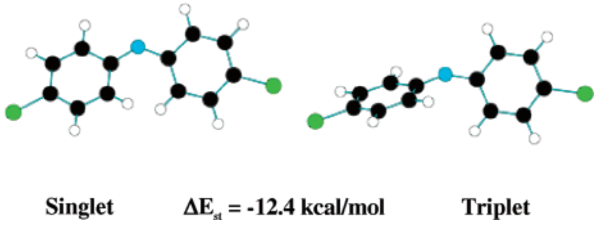

The reactive intermediates *N*,*N*-di(4-chlorophenyl)nitrenium ion and *N*,*N*-di(4-bromophenyl)nitrenium ion were generated through photolysis of the corresponding *N*-amino(2,4,6,-collidinium) ions. The behavior of these diarylnitrenium ions was characterized by laser flash photolysis, analysis of the stable photoproducts, and ab initio calculations with density functional theory. The latter predict these species to have singlet ground states. The halogenated diarylnitrenium ions are significantly longer lived than the unsubstituted diphenylnitrenium ion. Specifically, cyclization to form carbazole derivatives occurs negligibly, if at all, with the halogenated derivatives. They do, however, carry out most of the characteristic reactions of singlet arylnitrenium ions, including combining with nucleophiles on the aryl rings, adding to arenes, and accepting electrons from readily oxidized traps. Interestingly these species also abstract H atoms from 1,4-cyclohexadiene and various phenol derivatives. The implication of the latter process in relation to the computed singlet−triplet energy gaps of ca. −12.5 kcal/mol is discussed.

Introduction

Nitrenium ions are highly reactive intermediates that are structurally characterized by a dicoordinate nitrogen bearing a formal positive charge. Various substituted arylnitrenium ions have been shown to be intermediates in DNA-damaging reactions caused by metabolically activated amines.[1−12] Other examples of this class of reactive intermediates are proposed to be involved in the synthesis of the conducting polymer, poly(aniline).[13,14] However, recently several investigators have begun to explore applications of nitrenium ions to synthetically useful cyclization reactions.[15] Nitrenium ions have low-energy singlet and triplet electronic states. The aryl derivatives are generally ground state singlets, although it appears that appropriately substituted arylnitrenium ions can be ground state triplets.[16−23]

---

* Address correspondence to this author. Fax: 301-314-9121.

(1) Miller, E. C.; Miller, J. A. *Pharmacol. Rev.* **1966**, *18*, 805.

(2) Miller, E. C.; Lotlikar, P. D.; Miller, J. A.; Butler, B. W.; Irving, C. C.; Hill, J. T. *Mol. Pharmacol.* **1968**, *4*, 147.

(3) Miller, J. A.; Miller, E. C. Physico-Chemical Mechanisms of Carcinogenesis. In *Jerusalem Symposia on Quantum Chemistry and Biochemistry*; The Israel Academy of Sciences and Humanities: Jerusalem, 1969; Vol. 1, p 237.

(4) Poirier, L. A.; Miller, J. A.; Miller, E. C.; Sato, K. *Cancer Res.* **1967**, *27*, 1600.

(5) Cramer, J. W.; Miller, J. A.; Miller, E. C. *J. Biol. Chem.* **1960**, *235*, 885.

(6) Novak, M.; Kennedy, S. A. *J. Phys. Org. Chem.* **1998**, *11*, 71.

(7) Novak, M.; Kennedy, S. A. *J. Am. Chem. Soc.* **1995**, *117*, 574.

(8) Humphreys, G. W.; Kadlubar, F. F.; Guengerich, F. P. *Proc. Natl. Acad. Sci.* **1992**, *89*, 8278.

(9) McClelland, R. A.; Ahmad, A.; Dicks, A. P.; Licence, V. E. *J. Am. Chem. Soc.* **1999**, *121*, 3303.

(10) Kriek, E. *Biochim. Biophys. Acta* **1974**, *355*, 177.

(11) McClelland, R. A.; Gadosy, T. A.; Ren, D. *Can. J. Chem.* **1998**, *76*, 1327.

(12) McClelland, R. A.; Kahley, M. J.; Davidse, P. A. *J. Phys. Org. Chem.* **1996**, *9*, 355.

(13) Ding, Y.; Padias, A. B.; Hall, H. K. *J. Polym. Sci. Part A: Polym. Chem.* **1999**, *37*, 2569.

(14) Wei, Y.; Jang, G. W.; Chan, C. C.; Hsueh, K. F.; Hariharan, R.; Patel, S. A.; Whitecar, C. K. *J. Phys. Chem.* **1990**, *94*, 7716.

(15) Abramovitch, R. A.; Miller, J.; de Souza, A. J. C. *Tetrahedron Lett.* **2003**, *44*, 6965.

(16) Falvey, D. E. In *Organic, Physical and Materials Photochemistry*; Ramamurthy, V. S., Schanze, K., Eds.; Marcel Dekker: New York, 2000.

(17) Falvey, D. E. *J. Phys. Org. Chem.* **1999**, *12*, 589.

10.1021/jo062578i CCC: $37.00

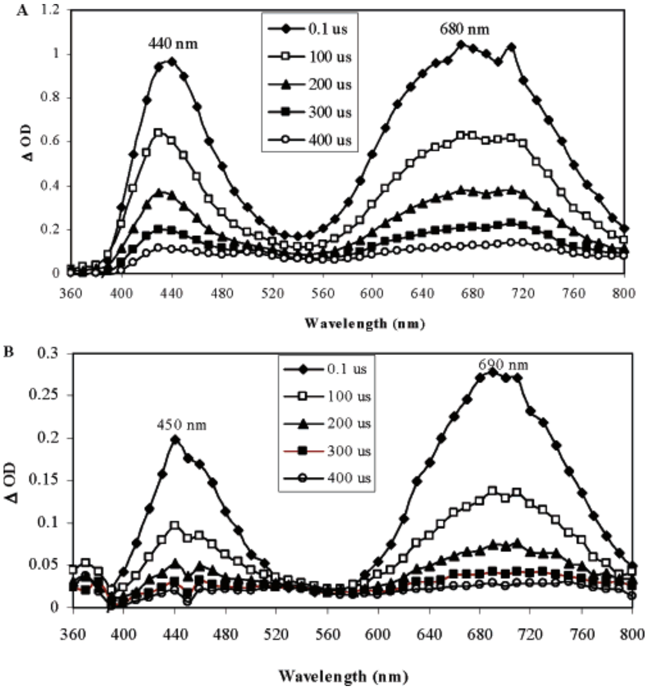

FIGURE 1. Transient spectra obtained upon photolysis of (A) **1b** and (B) **1c** in CH_3CN.

The chemical and spectroscopic behavior of diphenylnitrenium ion **2a** was described in several earlier articles.[21,24−26] This intermediate can be generated through photolysis of 1-(*N*,*N*-diphenylamino)-2,4,6-triphenylpyridinium ion. Several decay pathways were characterized including the following: (1) a coupled deprotonation/electrocyclization reaction, forming carbazole, (2) addition of simple nucleophiles (water alcohols, halide ions) to the ring carbons, (3) addition of electron-rich aromatics to the nitrogen as well as the para and ortho ring positions, and (4) abstraction of hydride from suitable donors.

The following study was undertaken to ascertain the effects of ring halogenation on the behavior of diarylnitrenium ions. It is shown that these species are much more stable with respect to the aforementioned deprotonation/electrocyclization process and addition of the simple nucleophiles compared with Ph_2N^+. The reactivity toward electron-rich arenes is found to be undiminished. Calculations with density functional theory (B3LYP) on the 4,4′-dihalo-derivatives predict that they are ground state singlets. However, LFP experiments show that they carry out a net H atom abstraction from several traps, a reaction pathway that has been previously only associated with the triplet state.

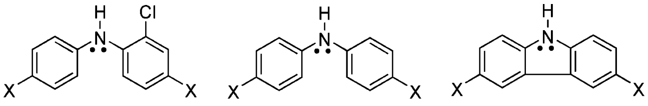

4b X = Cl
c X = Br

5b X = Cl
c X = Br

6b X = Cl
c X = Br

FIGURE 2. Photoproducts isolated from the photolysis of **1** in the presence of chlorides.

Results and Discussions

***N*-(4,4′-Dichlorodiphenyl) and *N*-(4,4′-Dibromodiphenyl) Nitrenium Ions.** *N*-(4,4′-dichlorodiphenylamino)-2,4,6-trimethylpyridinium **1b** and *N*-(4,4′-dibromodiphenylamino)-2,4,6-trimethylpyridinium ion **1c** (BF_4^- salts) are the two *N*-aminopyridinium salts used in our work to generate the nitrenium ions of interest. Upon photolysis, the N−N bond is cleaved heterolytically to generate the nitrenium ion (Scheme 1).

The halogenated diarylpyridinium salts, **1b** and **1c**, were synthesized by adapting a previously described route. The respective hydrazines are combined with substoichiometric amounts of 2,4,6-trimethylpyrylium tetrafluoroborate to yield the corresponding **1b** and **1c**. The hydrazines are synthesized via nitrosation of the halogenated diphenylamines followed by reduction with zinc. Dichlorodiphenyl amine was synthesized by using the Goldberg procedure and the bromination of diphenylamine is accomplished by refluxing the *N*-benzoyldiphenylamine with Br_2 in CH_2Cl_2.[27−29]

Laser flash photolysis was used to characterize the spectra and lifetimes of nitrenium ions, **2b** and **2c**. Pulsed laser (355 nm,25 mJ, 6 ns) photolysis of **1b** and **1c** in CH_3CN (N_2 purged) generates two strong transient absorption bands (**1b**: 440, 680 nm; **1c**: 450, 690 nm), which appear immediately following the excitation pulse and decay with first-order lifetimes of 240 (**2b**) and 124 μs (**2c**) (Figure 1). These bands are attributed to the halogenated diarylnitrenium ions **2b** and **2c** (Scheme 1). Carrying out the photolysis in CH_2Cl_2 or in the presence of oxygen did not affect the transient absorption or the lifetime of the transient species observed in Figure 1.

To verify the assignment of the absorption bands in Figure 1, calculations on the structures of **2b** and **2c** were carried out with density functional theory (DFT). Specifically the geometries of both the singlet and triplet states were optimized at the B3LYP/6-31G(d,p) level and detailed results are presented in the Supporting Information (Figure S1). As seen with previous arylnitrenium ions, the triplet states are characterized by wider central (C−N−C) bond angles (ca. 150°) compared with the singlet states (ca. 126°).[16,18,20,30] Likewise the singlets have nearly coplanar phenyl rings (dihedral 36°) compared with the triplets, where the rings are nearly orthogonal (dihedral ca. 98°). Qualitatively, these geometric differences can be understood to arise from maximization of overlap between the unfilled nitrogen based p-orbital and the filled π-orbitals on the aryl rings in the case of the singlet.

Time dependent−density functional theory (TD-DFT) calculations were carried out on the singlet and triplet states of

---

(18) Falvey, D. E.; Cramer, C. J. *Tetrahedron Lett.* **1992**, *33*, 1705.

(19) Chiapperino, D.; Anderson, G. B.; Robbins, R. J.; Falvey, D. E. *J. Org. Chem.* **1996**, *61*, 3195.

(20) Sullivan, M. B.; Brown, K.; Cramer, C. J.; Truhlar, D. G. *J. Am. Chem. Soc.* **1998**, *120*, 11778.

(21) Srivastava, S.; Ruane, P. H.; Toscano, J. P.; Sullivan, M. B.; Cramer, C. J.; Chiapperino, D.; Reed, E. C.; Falvey, D. E. *J. Am. Chem. Soc.* **2000**, *122*, 8271.

(22) Srivastava, S.; Toscano, J. P.; Moran, R. J.; Falvey, D. E. *J. Am. Chem. Soc.* **1997**, *119*, 11552.

(23) Srivastava, S.; Falvey, D. E. *J. Am. Chem. Soc.* **1995**, *117*, 10186.

(24) Moran, R. J.; Falvey, D. E. *J. Am. Chem. Soc.* **1996**, *118*, 8965.

(25) McIlroy, S.; Moran, R. J.; Falvey, D. E. *J. Phys. Chem. A* **2000**, *104*, 11154.

(26) Kung, A. C.; McIlroy, S.; Falvey, D. E. *J. Org. Chem.* **2005**, *70*, 5283.

(27) Freeman, H. S.; Butler, J. R.; Freedman, L. D. *J. Org. Chem.* **1978**, *443*, 4975.

(28) Winter, A. H.; Thomas, S. I.; Kung, A. C.; Falvey, D. E. *Org. Lett.* **2004**, *6*, 4671.

(29) Moran, R. J. Ph. D. Dissertation, University of Maryland, 1997.

(30) Cramer, C. J.; Falvey, D. E. *Tetrahedron Lett.* **1997**, *38*, 1515.

SCHEME 1. Photolysis of Pyridinium Salt Precusor to Generate Nitrenium Ions

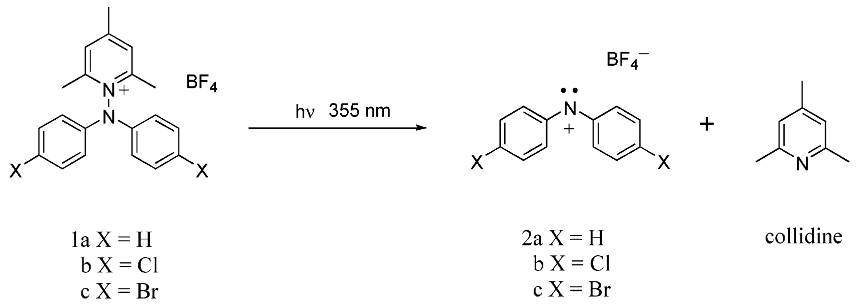

SCHEME 2. Nucleophilic Addition Pathway to 2

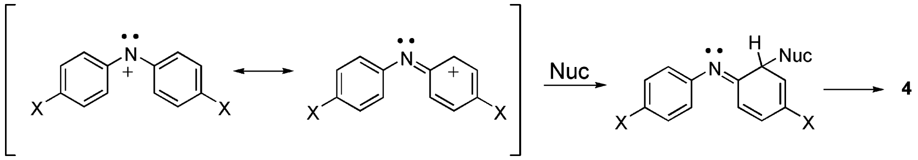

SCHEME 3. Proposed Radical Coupling Pathway Leading to 9

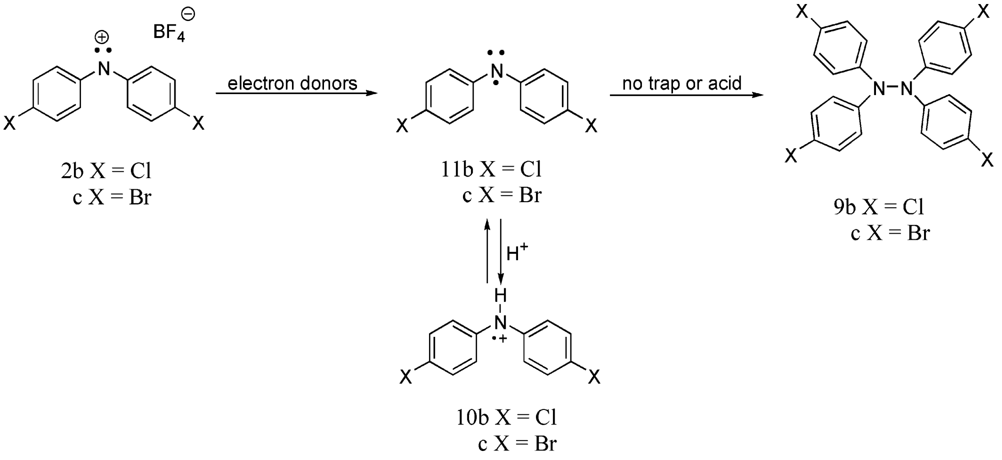

TABLE 1. Calculated Energy Gap and Experimental Data for 2a, 2b, and 2c

		absorption (nm)			
nitrenium ions	ΔE_{ST} (kcal/mol)	calcd singlet	calcd triplet	exptl	lifetimes τ (ms)
2a	−11.2			425, 680	1.5 (CH_3CN)
2b	−12.7	465, 637	589 (weak)	440, 680	240 (CH_3CN) 8.47 (H_2O)
2c	−12.4	465, 647	580 (weak)	450, 690	124 (CH_3CN) 6.57 (H_2O)

the two nitrenium ions in order to predict their UV−vis spectra. The singlet states are calculated to have two strong absorption bands in the visible region: (1) a high wavelength transition corresponding to a transition from the nonbonding pair on the nitrogen to the LUMO, which is a mixture of the nitrogen-based p-orbital and corresponding π-orbitals on the aryl rings and (2) at lower wavelengths, two $\pi-\pi^*$ transitions separated by ca. 5 nm, one allowed and one forbidden. The triplets show a single weak transition from what are primarily aryl-based π-orbitals to the semioccupied sp^2-like orbital on nitrogen.

As seen in Table 1, the experimental data are clearly more consistent with the predicted singlet spectra. Furthermore, the ΔE_{ST} values obtained by DFT calculations predict that the singlet state of **2b** and **2c** is lower in energy than the triplet state by ca. 12.5 kcal/mol. The ΔE_{ST} values for most arylnitrenium ions previously studied are in the range of −11 to −18 kcal/mol and all these ions have been proven to be ground state singlets.[16]

Stable photoproducts. Photolysis of **1b** and **1c** under conditions where nucleophilic traps are present yields stable photoproducts that are consistent with intermediate formation of the nitrenium ions **2**. For example, in the presence of chloride ion, photolysis of **1b** and **1c** yields three photoproducts: ortho adduct **4**, parent amine **5**, and carbazole **6** (Figure 2). Compounds **4** and **5** are obtained in a 1:1 mol ratio with trace amounts of **6**. Compound **4** is obtained as a result of addition of chloride to the ortho carbon of one of the phenyl ring as shown in Scheme 2. Generally the positive charge in a diarylnitrenium ion is either localized on the nitrogen or delocalized to the ortho or para carbon of one of the phenyl rings resulting in the addition of the nucleophile to the nitrogen or the phenyl ring. In the case of **2b** and **2c**, only compound **4** is observed, *N* adducts or para adducts are not observed. The absence of the para adduct could be due to the fact that the chloride ion adds reversibly to the para carbon, whereas the ortho addition can be followed by deprotonation to provide the product. A similar product study conducted on **2a** in the presence of chloride yielded both para and ortho adducts. The para

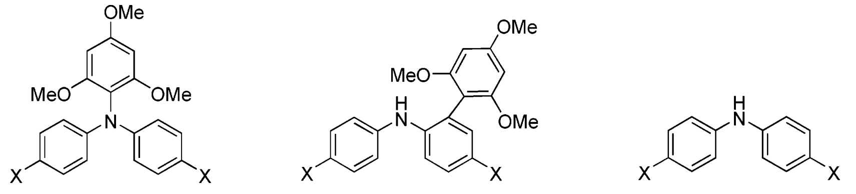

7b X = Cl
c X = Br

8b X = Cl
c X = Br

5b X = Cl
c X = Br

FIGURE 3. Photoproducts obtained from the photolysis of **1** in the presence of 1,3,5-TMB.

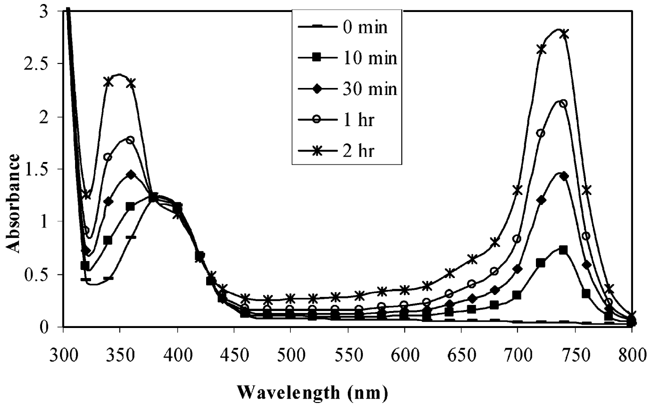

FIGURE 4. UV absorption spectra for the photolysis of **1b** in CH_2Cl_2 with TFA.

position in **2a** is not substituted; hence nucleophilic addition at that site is possible.

In addition to the ortho adduct, compounds **5** and **6** are also obtained. Even though these compounds are not the result of the nucleophilic addition process, they are still consistent with formation of a cationic intermediate. The formation of **5** from **2** requires the net addition of 2 electrons and a proton to the latter. There are two mechanisms that could lead to this result. The first would be one-electron oxidation of chloride followed by a subsequent H atom (or electron) transfer to the resulting aminyl radical. Another possibility is an inner-sphere electron-transfer mechanism similar to one proposed by Novak.[31] In this pathway a halide adds to the nitrenium ion and is then displaced by a second halide or other nucleophile, resulting in a net 2-electron reduction of the nitrenium ion. The carbazole derivatives, **6**, are interesting, but are obtained only in trace amounts. We assume that these are derived from secondary photolysis of **5**.

Also examined were reactions of **2b** and **2c** with 1,3,5-TMB. Previous studies have shown that these nucleophiles react rapidly with diarylnitrenium ions to yield σ-adducts. Similar σ-addition products are observed for **2b** and **2c** except that no para adduct is obtained. Photolyzing **1b** and **1c** in the presence of 0.02 M 1,3,5-TMB in CH_3CN also yields three photoproducts: *N*-adduct **7**, ortho adduct **8**, and the parent amine **5** in a 2:2.5:1 mol ratio (Figure 3). TMB adds either to the nitrogen or the ortho carbon of the phenyl ring.

Reaction in the Absence of Traps. In the absence of any traps, diphenylnitrenium ion **2a** decays to yield carbazole and a significant amount of dimeric and oligomeric products arising from the oxidation of the parent amine. Carbazole formation occurs through the intramolecular cyclization of **2a**. In contrast, the halogenated derivatives photolyze to cleanly provide the symmetric dimer **9**, along with collidine.

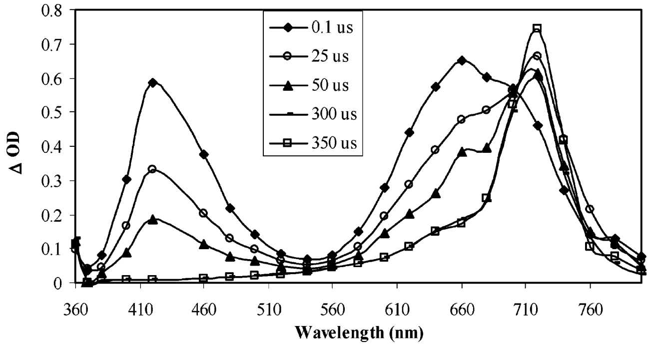

FIGURE 5. Transient spectra of the photolysis of **1b** in CH_3CN with 10% H_2SO_4.

The photolysis of **1b** and **1c** in CD_3CN was carried out under room light and followed by ^{1}H NMR every 20−30 min. As the photolysis progressed, the gradual depletion of the pyridinium precursor and the growth of hydrazine derivative **9** along with collidine is observed. Compound **9** was isolated and characterized by ^{1}H NMR, ^{13}C NMR, and MS. To form **9** from **2b** or **2c**, the nitrenium ion would have to abstract an electron before dimerizing (Scheme 3). Taking into account the fact that **2b** and **2c** are relatively long-lived in most solvents and that dimer forms in the absence of any traps, we assumed that it might be possible to observe the nitrenium ion by steady-state UV if dimerization could be suppressed. Therefore, we investigated the possibility of stabilizing the nitrenium ion generated by photolysis in solvents incapable of donating electrons.

The photolysis was performed by dissolving **1b** and **1c** in different solvents with acid (H_2SO_4 or trifluoroacetic acid (TFA)) and photolyzing under room light. The solvents chosen for steady state analysis are not considered to be efficient H-atom or electron donors (CH_2Cl_2, nitrobenzene, and chlorobenzene). The UV−vis spectra taken during the course of the photolysis in CH_2Cl_2 are shown in Figure 4. A sharp absorption band with maxima at 740 nm for **1b** and 750 nm for **1c** develops and is stable for up to 2 h. This signal is attributed to the radical cation (**10**) of **5**. Similar steady-state UV spectra are obtained in nitrobenzene and chlorobenzene (figures are given in the Supporting Information). More detail about the identity of **10** will be discussed later.

The experiment is repeated by LFP where **1b** is photolyzed in CH_3CN with 10% H_2SO_4. Transient spectra obtained in this manner are shown in Figure 5. Upon photolysis, the signals corresponding to **2** cleanly decay in favor of a new long-lived species absorbing at 720 nm, which is then attributed to **10**. (The small, quantitative discrepancy in maxima is attributed to

---

(31) Pelecanou, M.; Novak, M. *J. Am. Chem. Soc.* **1985**, *107*, 4499.

TABLE 2. Second-Order Rate Constants (k_{nuc}) for the Reaction of 2 with Nucleophiles in CH_3CN

	k_{nuc} (M^{-1} s^{-1})		
traps	**2a**	**2b**	**2c**
$Cl^{-\,a}$	$1.0 \times 10^{10\,b}$	$(1.06 \pm 0.03) \times 10^{10}$	$(9.83 \pm 0.60) \times 10^{9}$
H_2O	$6.1 \times 10^{5\,b}$	$(1.51 \pm 0.16) \times 10^{4}$	$(1.12 \pm 0.01) \times 10^{4}$
MeOH	$5.2 \times 10^{6\,b}$	$(1.07 \pm 0.12) \times 10^{5}$	$(7.74 \pm 0.48) \times 10^{4}$
EtOH	$4.9 \times 10^{6\,b}$	$(1.05 \pm 0.08) \times 10^{5}$	$(8.18 \pm 0.59) \times 10^{4}$
2-propanol		$(4.28 \pm 0.38) \times 10^{4}$	$(2.30 \pm 0.61) \times 10^{4}$
dGMP[c]		$(5.56 \pm 0.41) \times 10^{8}$	$(7.65 \pm 0.20) \times 10^{8}$

[a] nBu_4NCl is the source for Cl^-. [b] Reference 24. [c] Deoxyguanosine 5′-monophosphate disodium salt in 9:1 buffer (PO_4^{-3}, 25 mM)/CH_3CN.

differences in the solvent.) On the basis of these observations we conclude that, in the absence of efficient nucleophilic traps, the nitrenium ion ultimately accepts an electron and dimerizes. The radical coupling step of intermediate radical **11** can be suppressed by protonating the latter with strong acids. Under such circumstances, the cation radicals persist. Less clear is the source of reducing equivalents. It would seem improbable that solvents such as nitrobenzene or methylene chloride and/or the acids could function in this capacity. At this point we assume that trace impurities in these media are serving as the source of the reducing equivalents. However, additional studies aimed at clarifying this are planned.

Kinetic Analysis: Trapping with Simple Nucleophiles. Along with product studies, the trapping rate constants of **2b** and **2c** by various nucleophiles were measured. LFP was used to obtain the pseudo-first-order decay rate constants (k_{obs}) of **2b** and **2c** in varying concentrations of a particular nucleophile at a specific wavelength (680 or 690 nm). The k_{obs} thus obtained is applied to eq 1 and the quenching rates by nucleophiles are obtained as a second-order rate constant (k_q). k_o is the k_{obs} in the absence of nucleophile and Q is the concentration of the nucleophile.

$$k_{obs} = k_o + k_q[Q] \tag{1}$$

Table 2 shows that **2b** and **2c** react with H_2O and alcohols much more slowly than **2a**, whereas chloride quenches **2b** and **2c** at the diffusion limit. H_2O and alcohols are weaker nucleophiles than Cl^- thus their reactivity toward nitrenium ions shows a greater dependence upon the stability of the nitrenium ion. In the reaction of **2a** with CH_3OH, the $-OCH_3$ group adds to the para position of the phenyl ring rather than the ortho position.[24] Similar addition is not possible for **2b** and **2c** because the para position is blocked by the halogens, thus reducing the reactivity.

The low reactivity of **2b** and **2c** toward H_2O makes it possible to characterize their lifetimes and reaction rate constants in aqueous media. One of the more noteworthy reactions of mono-arylnitrenium ions (e.g., 2-fluorenylnitrenium ion) is their rapid reactions with DNA bases, specifically with guanine.[6,11,32] There is a considerable body of evidence suggesting that the genotoxicity of arylnitrenium ions is related to their ability to react rapidly with DNA balanced by their ability to survive in an aqueous medium long enough to react with DNA.[11,33] This encouraged us to examine the reactions of the diarylnitrenium ions with 2′-deoxyguanosine monophosphate (dGMP) in aqueous media using LFP. As shown in Table 2, the diarylnitrenium ions do react with dGMP, but with rate constants that are approximately 10-fold lower than what has been reported for carcinogenic mono-aryl derivatives.[34] No additional intermediates were detected in these experiments. The aminyl radical generated from electron abstraction would have been detected at 760 nm (see the Supporting Information, Figure S8). On the other hand, the intermediates arising from direct addition to the C-8 position, as observed by McClelland et al., would likely have been obscured by depletion of the *N*-aminopyridinium precursor.[9,11] Thus we cannot make any definitive conclusions about the detailed mechanism of this process.

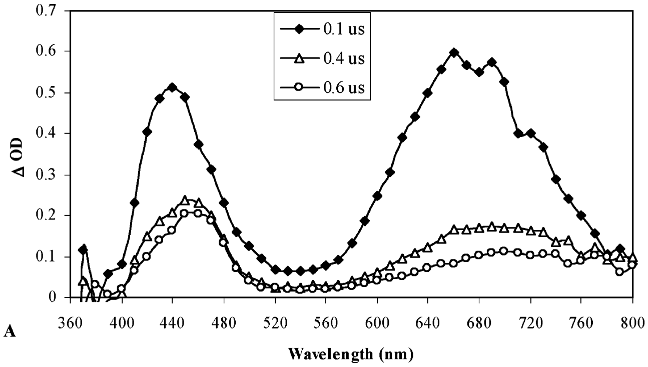

FIGURE 6. Transient spectra of the photolysis of **1b** in the presence of *N*,*N*-DMA.

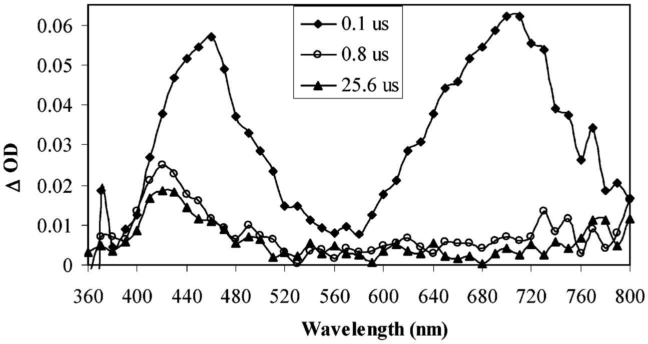

FIGURE 7. Transient spectra from the photolysis of **1c** in the presence of 1,3,5-TMB.

Trapping with π-Nucleophiles. Transient spectra obtained by LFP show that readily oxidized arenes, namely, *N*,*N*-dimethylaniline (*N*,*N*-DMA), 1,4-dimethoxybenzene (1,4-DMB), hexamethylbenzene (HMB), and 4-methylanisole (4-MA), react with **2b** and **2c** via an electron-transfer process. Figure 6 illustrates the results of LFP generation of **2b** and **2c** in the presence of *N*,*N*-DMA. The absorption bands of the nitrenium ions decay rapidly in favor of two longer lived absorption bands: a strong band at 460 nm and a weak broad signal at 760 nm. The former is readily assigned to the cation radical of *N*,*N*-DMA on the basis of literature precedent.[35] The latter is ascribed to the neutral radical **11** arising from one-electron reduction of the diarylnitrenium ion.

Verification of the assignment of the 760 nm signals to **11** was done by generating the same radicals via an independent route. Following a general procedure described by Lustzyk et

---

[32] Novak, M.; Lin, J. J. *J. Am. Chem. Soc.* **1996**, *118*, 1302.

[33] Davidse, P. A.; Kahley, M. J.; McClelland, R. A.; Novak, M. *J. Am. Chem. Soc.* **1994**, *116*, 4513.

[34] Chiapperino, D.; McIlroy, S.; Falvey, D. E. *J. Am. Chem. Soc.* **2002**, *124*, 3567.

[35] Shida, T. *Electronic Absorption Spectra of Radical Ions*; Elsevier: Amsterdam, The Netherlands, 1988.

SCHEME 4. Generation of Aminyl Radicals 11 from *N*-Nitrosoamine

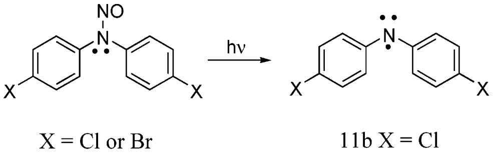

11b X = Cl
c X = Br

al., LFP was carried out on 1,1′-di(4-chlorophenyl)nitrosoamine and 1,1′-di(4-bromophenyl)nitrosoamine[36] (Scheme 4). In both cases, broad absorption bands at 760 nm are observed that are indistinguishable from the absorptions generated from the *N*,*N*-DMA trapping experiments.

Similar behavior is seen with 1,4-DMB, MA, and HMB. These arenes react with **2b** and **2c** to produce radical intermediates. Table 3 lists these results. In these cases a sharper transient signal at 720 nm due to the cation radical of the diarylamine (**10**) results from the subsequent protonation of **11**. Because these arenes are not as basic as DMA, any protons are capable of adding to the radical **11**. The identity of the cation radical (**10)** was also confirmed by independent generation; in this case we carried out LFP of the amines **5** in the presence of the electron acceptor, 1,4-dicyanobenzene (Scheme 5). The cation radicals of the traps were identified by their previously characterized absorption bands.

No change in the lifetime of **1b** or **1c** was observed upon addition of *p*-xylene, 4-bromoanisole, and 4-chloroanisole. These have oxidation potentials >1.7 V vs SCE so we conclude that they are incapable of reducing the nitrenium ions at a measurable rate.

Two arenes 1,3-DMB and 1,3,5,-TMB also react rather rapidly with the nitrenium ions. In these cases, new intermediates are detected, in each case showing an apparent maximum at 410 nm (Figure 7). Previously it was reported that **2a** reacts with these same arenes to provide σ-complexes[37] (Scheme 6). The latter had apparent absorption maxima near 350 nm. In the present case the apparent maxima are at higher wavelengths. However, it should be noted that the observed peaks occur near the onset of absorption of the photoreactants (**1**). Thus photobleaching due to depletion of **1** may distort the maxima from their true values. Further support for the assignment comes from quenching experiments. In the earlier example the σ-complexes were shown to be deprotonated by added base (pyridine). Likewise in the present case the lifetimes of the assigned σ-complexes (**12**) are diminished when the LFP experiments are carried out with added pyridine (0.41 mM) (Figure 8).

Trapping with Hydrogen Atom Donors. In previous studies we have argued that H atom abstraction is a characteristic reaction of the triplet state of arylnitrenium ions. For example, the yields of stable products derived from H atom transfer increase when the nitrenium ions are generated through triplet sensitization, rather than direct photolysis. In some cases the intermediate cation radicals have been detected. In the case of **2a**, where the nitrenium ion is known to be formed in the singlet state and that state is clearly the ground state, apparent products of H atom transfer were attributed to hydride, rather than H atom transfer.[25]

Similar H atom trapping experiments were carried out wherein **2b** and **2c** were generated in the presence of various H atom donors. As summarized in Table 4, 1,4-cyclohexadiene, cycloheptatriene, and various phenol derivatives all trap these nitrenium ions with rate constants in range of 10^5 to 10^6 M^{-1} s^{-1}. More significantly examination of the transient spectra following photolysis shows that the corresponding amine cation radical **10** (720 nm) forms concurrently with the decay of **2**. Figure 9 illustrates a typical case. Clearly, the H atom transfer process is the net result of these reactions. It is of course possible that the same intermediate could be derived from a sequential electron and proton transfer. However, in that case we would expect the rate constants to depend on the oxidation potential of the donor. (Recall that arenes with $E_{ox} > 1.7$ V were unreactive toward the same nitrenium ions.) In fact 4-cyanophenol ($E_{ox} = 2.5$ V) reacts with a rate constant that is only slightly diminished relative to that of phenol ($E_{ox} = 2.1$ V). A kinetic isotope effect study provides further evidence favoring direct H atom transfer rather than electron transfer. Specifically we compared the quenching of both **2b** and **2c** with phenol (OH) and phenol (OD) with use of LFP. These experiments provide a $k_H/k_D = 1.32$.

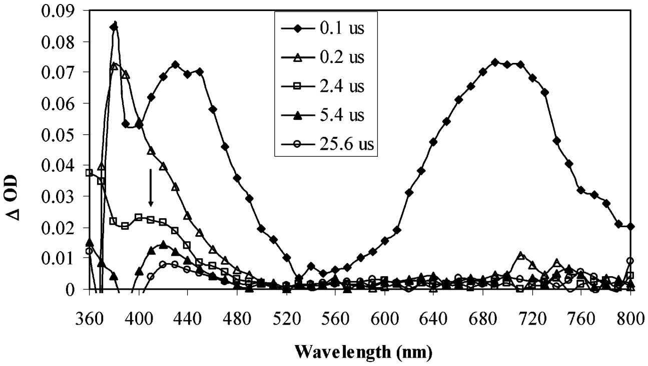

FIGURE 8. Transient spectra of the photolysis of **2c** in the presence of 1,3,5-TMB (11.8 mM) and pyridine (0.41 mM).

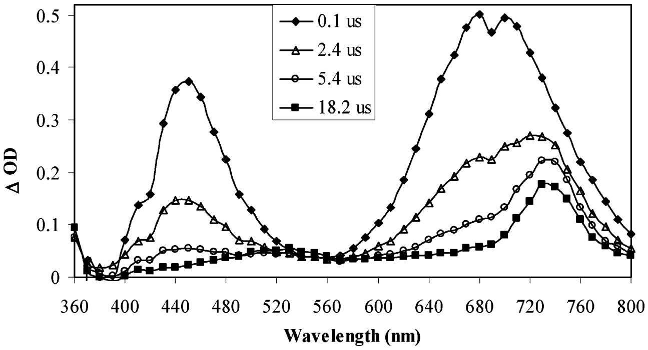

FIGURE 9. Transient spectra of the photolysis of **1c** in the presence of 1,4-CHD in CH_3CN.

To determine the stable products formed in these reactions, a CD_3CN solution of **1c** (1 mM) was photolyzed in the presence of 12 mM CHD. Analysis of the photolysis mixture by ^1H NMR showed clean formation of the amine **5c** along with collidine, benzene, and unreacted CHD. No other products were observed.

The apparent H atom abstraction by nitrenium ions **2b** and **2c** is somewhat unexpected. We are unaware of any examples of singlet state hypovalent intermediates (carbenes, nitrenes, etc.) abstracting H atoms to provide (cage-escaped) radical intermediates. The prevailing view is that singlet geminate radical pairs generated in such reactions subsequently form bonds in preference to escaping the solvent cage. The DFT calculations, which

---

[36] Wagner, B. D.; Ruel, G.; Lusztyk, J. *J. Am. Chem. Soc.* **1996**, *118*, 13.

[37] McIlroy, S.; Falvey, D. E. *J. Am. Chem. Soc.* **2001**, *123*, 11329.

SCHEME 5. Generation of Cation Radicals 11

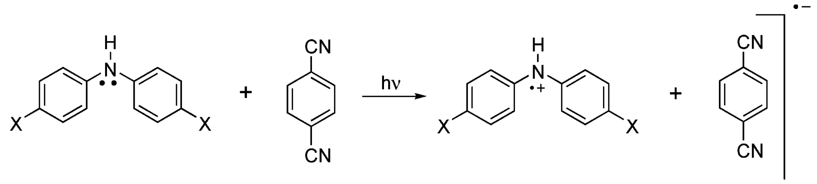

5b X = Cl
c X = Br

1,4-DCB

11b X = Cl
c X = Br

SCHEME 6. Addition of 2 to 1,3,5-TMB via a σ-Complex 12

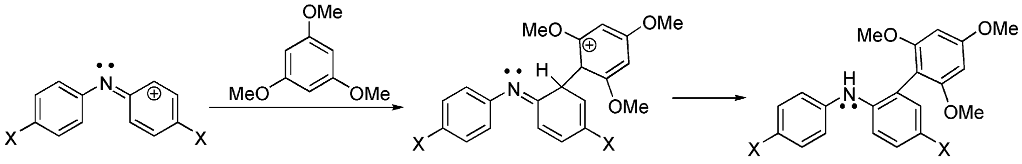

12b X = Cl
c X = Br

8b X = Cl
c X = Br

TABLE 3. Second-Order Rate Constants (k_{nuc}) for the Reaction of 2 with Electron Donors in CH_3CN

		2b		**2c**	
traps	E_{ox} (V vs SCE)	k_{nuc} (M^{-1} s^{-1})	intermediates upon quenching (nm)	k_{nuc} (M^{-1} s^{-1})	intermediates upon quenching (nm)
N,*N*-DMA	0.53	$(5.06 \pm 0.20) \times 10^9$	760 (**11**)	$(6.01 \pm 0.40) \times 10^9$	760 (**11**)
1,4-DMB	1.34	$(2.45 \pm 0.14) \times 10^7$	720 (**10**)	$(4.03 \pm 0.23) \times 10^7$	730 (**10**)
hexamethylbenzene	1.62	$(8.08 \pm 0.40) \times 10^6$	720 (**10**)	$(7.46 \pm 0.12) \times 10^6$	730 (**10**)
4-methylanisole	1.64	$(3.14 \pm 0.40) \times 10^5$	720 (**10**)	$(2.45 \pm 0.11) \times 10^5$	730 (**10**)
4-bromoanisole	1.78	no trapping		no trapping	
4-chloroanisole	2.00	no trapping		no trapping	
p-xylene	2.01	no trapping		no trapping	
1,3-DMB	1.49	$(2.45 \pm 0.08) \times 10^8$	410 (σ-adduct)	$(4.21 \pm 0.75) \times 10^8$	410 (σ-adduct)
1,3,5-TMB	1.49	$(1.34 \pm 0.09) \times 10^9$	420 (σ-adduct)	$(5.17 \pm 0.24) \times 10^9$	420 (σ-adduct)

TABLE 4. Second-Order Rate Constants (k_{nuc}) for the Reaction of 2 with Hydrogen Atom Donors in CH_3CN

			k_q (M^{-1} s^{-1})		
trap	E_{ox} (V)	BDE (kcal/mol)	**2a**	**2b**	**2c**
1,4-cyclohexadiene	1.74	76.6 ± 1.2	$(6.5 \pm 0.2) \times 10^6$	$(5.86 \pm 0.31) \times 10^6$	$(5.13 \pm 0.15) \times 10^6$
cycloheptatriene	1.43	76.6 ± 3	$(1.4 \pm 0.1) \times 10^7$	$(5.65 \pm 0.14) \times 10^6$	$(5.99 \pm 0.67) \times 10^6$
phenol	2.10	90.4 ± 1		$(6.81 \pm 0.22) \times 10^5$	$(6.46 \pm 0.95) \times 10^5$
4-bromophenol	2.18	90.7		$(3.76 \pm 0.33) \times 10^5$	$(4.73 \pm 0.37) \times 10^5$
4-cyanophenol	2.57	94.2		$(3.31 \pm 0.89) \times 10^5$	$(4.89 \pm 0.87) \times 10^5$

are validated by successful TD-DFT predictions of the UV−vis spectra, show that **2b** and **2c** are ground state singlets with substantial energy gaps. The LFP detection of the singlet nitrenium ions prior to formation of the radical cations militate against H atom abstraction by a higher energy unequilibrated triplet state generated in the photolysis. This leaves three possible explanations. First, it is possible that the DFT method systematically overestimates ΔE_{st}. Assuming diffusion-limited H atom abstraction by the triplet and a rapid singlet−triplet equilibrium, the rate constants in Table 1 would be consistent with $\Delta E_{st} = 4-6$ kcal/mol, which is ca. 6−8 kcal/mol lower than the computed values (Scheme 7). Alternatively, H atom transfer could be occurring via the singlet state through state mixing in the transition state. An analogous mechanism has been previously invoked to rationalize the reaction of ground-state triplet diarylcarbenes with methanol (a singlet state trap).[38,39] A state-mixing reaction pathway might demonstrate a heavy atom effect. In our case this would be manifested in higher H atom abstraction rate constants for the bromo derivative than the chloro derivative. Indeed, for 4 of the 5 traps examined the bromo derivative (**2c**) is found to be slightly more reactive than the chloro derivative. However, given its small magnitude, we consider this effect to be suggestive, rather than conclusive, evidence for the state mixing mechanism. Finally we note that the DFT methods employed here assume that the lowest singlet state has a closed shell (n^2) configuration. This is generally true for most carbenes as well as for NH_2^+. However, it has been demonstrated that the lowest singlet state of phenylnitrene actually has an open shell (n,p) configuration.[40,41] Thus, it is conceivable that H atom transfer might be occurring to an open shell singlet state diarylnitrenium ion. A more detailed examina-

---

(38) Griller, D.; Nazran, A. S.; Scaiano, J. C. *J. Am. Chem. Soc.* **1984**, *106*, 198−202.

(39) Rak, S. F.; Lapin, S. C.; Falvey, D. E.; Schuster, G. B. *J. Am. Chem. Soc.* **1987**, *109*, 5003−5008.

(40) Gritsan, N. P.; Zhu, Z.; Hadad, C. M.; Platz, M. S. *J. Am. Chem. Soc.* **1999**, *121*, 1202−1207.

(41) Hrovat, D. A.; Waali, E. E.; Borden, W. T. *J. Am. Chem. Soc.* **1992**, *114*, 8698−8699.

SCHEME 7. Reaction of Diarylnitrenium Ions with H Atom Donors

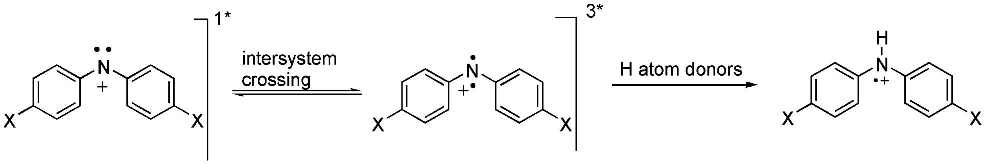

2b X = Cl
c X = Br

2b X = Cl
c X = Br

10b X = Cl
c X = Br

tion of the H atom transfer process and the electronic structures of the diarylnitrenium ions would be interesting.

Experimental Section

Calculations. The geometry optimization and vibrational frequency calculations reported in Table 1 were performed with the Gaussian 03 suite of programs. The calculations were done with use of the density functional theory, particularly the hybrid B3LYP functional that is comprised of Becke's B3 three parameter gradient-corrected exchange functional with the LYP correlation functional of Lee, Yang, and Parr that was originally described by Stephens et al.[42−45]

LFP Experiments. LFP studies were done with use of a Nd: YAG laser that uses harmonic generators to create an output wavelength of 266 or 355 nm. Transient absorption signal was obtained from the probe beam generated from a 350 W Xe arc lamp. Transient waveforms were captured on a digital oscilloscope with a bandwidth of 350 MHz at a rate of 1 point per 10 ns.

Samples used to generate the transient absorption spectra were prepared in distilled CH_3CN. A stock solution of the pyridinium salt is prepared in 150 mL of distilled CH_3CN with the concentration adjusted to have an optical density between 1.5 and 2.0 at 355 nm. The stock solution was purged with N_2 for at least 15 min before collecting data. The sample was photolyzed in a quartz cuvette. A fresh supply of the reaction mixture into the cuvette during experiment was attained by setting up a standard N_2 purged flow cell connecting the cuvette to the stock solution via a double-headed needle. This setup prevented the depletion of substrate and the accumulation of photoproducts during the experiment. Waveforms were collected for wavelengths ranging from 360 to 800 nm at an increment of 10 nm.

Kinetic studies were done by measuring the pseudo-first-order decay rate of the pyridinium salt in various concentrations of a quencher. A stock solution of the pyridinium salt is prepared in distilled CH_3CN to a concentration that has an optical density between 1.5 and 2.0 at 355 nm. A 3.0 mL portion of the stock solution is transferred to the quartz cuvette via a syringe. The pseudo-first-order decay rate of the transient species at a particular wavelength (**2b**: 680 nm; and **2c**: 690 nm) is obtained for varying concentrations of the quencher. At least five different concentrations, ranging from 0 to 1 mM, of the quencher are measured. The quenching rate is obtained as the slope by plotting the pseudo-first-order decay rate as a function of the quencher concentration.

Product Analysis with Chloride. A 50 mg portion of the pyridinium salt and 400 mg of NaCl are dissolved in 50 mL of 9:1 H_2O and CH_3CN. The reaction mixture is placed on the lab bench and photolyzed under room light. After photolysis, the mixture is neutralized with aqueous $NaHCO_3$. The organic layer is extracted. The aqueous layer is extracted with CH_2Cl_2 twice. The organic layers are combined and dried over $MgSO_4$. Upon filtration, the solvent is removed under reduced pressure to yield a brown oily residue. The photoproducts are isolated by preparative thin layer chromatography (20 × 20 plates; 1000 μm silica gel) with a mobile phase of 60:40 hexanes and ethyl acetate. Three photooproducts were isolated and characterized by ^{1}H NMR, ^{13}C NMR, and MS (DEI+): ortho adduct **4**, parent amine **5**, and 3,6-dihalogenated carbazole **6**. The halogenated carbazole had been observed and characterized previously.[46−48] **4b** (8.4 mg): ^{1}H NMR (400 MHz, CD_3CD) δ 7.45 (m, 1 H), 7.29 (d, J = 8.8 Hz, 2 H), 7.17 (m, 2H), 7.08 (d, J = 8.8 Hz, 2H), 6.58 (br, 1 H); ^{13}C NMR (400 MHz, CD_3CN) δ 141.7, 140.2, 130.2, 130.0, 129.9, 128.5, 127.3, 125.6, 124.0, 122.0, 119.0; MS (DEI+) *m/z* (rel intensity) 273.0 (100), 237.0 (14), 235.0 (12), 201.0 (60), 166.0 (11), 139.0 (9), 117.5 (12), 100.0 (7), 75.0 (9), 62.0 (5), 44.2 (4). **6b** (trace amounts): ^{1}H NMR (400 MHz, CD_3CD) δ 8.09 (d, J = 2.4 Hz, 2 H), 7.49 (d, J = 8.8 Hz, 2H), 7.41 (dd, J = 8.0, 2.4 Hz, 2H); ^{13}C NMR (400 MHz, CD_3CN) δ; MS (DEI+) *m/z* (rel intensity) 235.0 (100), 200 (40), 163.9 (22), 117.5 (20), 44.2 (25). **4c** (6.8 mg): ^{1}H NMR (400 MHz, CD_3CN) δ 7.57 (d, J = 2.4 Hz,1 H), 7.42 (d, J = 8.8 Hz, 2 H), 7.30 (dd, J = 8.8, 2.4 Hz, 1H), 7.13 (d, J = 8.8 Hz, 1H), 7.03 (d, J = 8.8 Hz, 2H), 6.59 (br, 1 H); ^{13}C NMR (400 MHz, CD_3CN) δ 142.2, 140.6, 133.1, 133.0, 131.5, 124.4, 122.4, 119.5, 114.8, 112.5; MS (DEI+) *m/z* (rel intensity) 360.8 (100), 316.9 (10), 245.0 (40), 201.0 (20), 166.1 (32), 139.0 (12), 100.5 (25), 75.0 (13), 63.0 (10), 50.0 (7). **6c** (trace amounts): ^{1}H NMR (400 MHz, CD_3CD) δ 8.24 (d, J = 2.0 Hz, 2 H), 7.53 (dd, J = 8.8, 2.0 Hz, 2H), 7.45 (d, J = 8.8, Hz, 2H); ^{13}C NMR (400 MHz, CD_3CN) δ MS (DEI+) *m/z* (rel intensity) 324.9 (100), 322.9 (55), 280.9 (10), 245.9 (18), 244.0 (15), 163.9 (18), 82.5 (10).

Product Analysis with 1,3,5-TMB. A 50 mg portion of the pyridinium salt and 169 mg of 1,3,5-TMB are dissolved in 50 mL of distilled CH_3CN. The reaction mixture is placed on the lab bench and photolyzed under room light. After photolysis, the mixture is shaken with equal amounts of deionized H_2O and CH_2Cl_2 and neutralized with saturated $NaHCO_3$. The extraction and characterization procedures are similar to those for NaCl. Three photoproducts are isolated and characterized by ^{1}H NMR, ^{13}C NMR, and MS (DEI+): *N* adduct **7**, ortho adduct **8**, and parent amine **5**. **7b** (12.6 mg): ^{1}H NMR (400 MHz, CD_3CD) δ 7.14 (d, J = 9.2 Hz, 4 H), 6.88 (d, J = 8.8 Hz, 4 H), 6.27 (s, 2H), 3.81 (s, 3H), 3.66 (s, 6H); ^{13}C NMR (400 MHz, CD_3CN) δ 162.5, 161.6, 159.4, 146.7, 129.5, 126.1, 122.1, 115.4, 92.4, 56.5, 56.1; MS (DEI+) *m/z* (rel intensity) 403.0 (25), 168.0 (100), 139.0 (65), 125.0 (20), 44.0 (12). **8b** (12.6 mg): ^{1}H NMR (400 MHz, CD_3CD) δ 7.19 (d, J = 2.4 Hz, 2H), 7.13 (d, J = 8.8 Hz, 2 H), 7.09 (m, 1H), 6.85 (d, J = 8.8 Hz, 2H), 6.26 (s, 2H), 5.89 (br, 1H), 3.81 (s, 3H), 3.62 (s, 6H); ^{13}C NMR (400 MHz, CD_3CN) δ 162.6, 159.4, 144.1, 141.6, 133.2, 129.6, 129.1, 128.2, 126.1, 124.8, 121.2, 119.2, 107.4, 56.3, 56.0; MS (DEI+) *m/z* (rel intensity) 403.6 (100), 344.6 (75), 337.5 (15), 203.4 (45), 183.4 (10), 42.2 (15), 28.1 (22). **7c** (25.1 mg): ^{1}H NMR (400 MHz, CD_3CD) δ 7.28 (d, J = 9.2 Hz, 4 H), 6.83 (d, J = 9.2 Hz, 4 H), 6.27 (s, 2H), 3.81 (s, 3H), 3.65 (s, 6H); ^{13}C NMR (400

---

(42) Becke, A. D. *Phys. Rev. A* **1988**, *38*, 3098.

(43) Becke, A. D. *J. Chem. Phys.* **1993**, *98*, 5648.

(44) Lee, C. T.; Yang, W. T.; Parr, R. G. *Phys. Rev. B* **1988**, *37*, 785.

(45) Stephens, P. J.; Devlin, F. J.; Chabalowski, C. F.; Frisch, M. J. *J. Phys. Chem.* **1994**, *98*, 11632.

(46) Chmielewski, M. J.; Charon, M.; Jurczak, J. *Org. Lett.* **2004**, *6*, 3501.

(47) Derosa, M.; Quesada, P. A.; Dodsworth, D. J. *J. Org. Chem.* **1987**, *52*, 173.

(48) Smith, K.; James, M. D.; Mistry, A. G.; Bye, M. R.; Faulkner, J. D. *Tetrahedron* **1992**, *48*, 7479.

MHz, CD_3CN) δ 162.5, 161.6, 159.4, 147.1, 132.5, 122.5, 113.5, 92.4, 56.5, 56.1; MS (DEI+) *m/z* (rel intensity) 493.0 (50), 168.0 (100), 139 (53), 125 (26), 44 (25). **8c** (34.5 mg): ^1H NMR (400 MHz, CD_3CD) δ 7.32 (dd, *J* = 8.0, 2.4 Hz, 1H), 7.26 (d, *J* = 8.8 Hz, 2 H), 7.23 (d, *J* = 2.8 Hz, 1 H), 7.16 (d, *J* = 8.4 Hz, 1H), 6.81 (d, *J* = 8.8 Hz, 2 H), 6.25 (s, 2H), 5.91 (br, 1H), 3.81 (s, 3H) 3.62 (s, 6H; ^{13}C NMR (400 MHz, CD_3CN) δ 162.6, 159.4, 144.4, 141.9, 136.1, 132.5, 131.1, 129.4, 121.5, 119.7, 113.5, 112.1, 107.4, 91.9, 56.3, 55.2; MS (DEI+) *m/z* (rel intensity) 493.0 (100), 491.0 (80), 381 (30), 338 (15), 59 (10), 44 (20).

Product Analysis in the Absence of Trap. A 50 mg portion of the pyridinium salt is dissolved in 50 mL of distilled CH_3CN. The reaction mixture is placed on the lab bench and photolyzed under room light. After photolysis, the mixture is neutralized with aqueous $NaHCO_3$. The organic layer is extracted. The aqueous layer is extracted with CH_2Cl_2 twice. The organic layers are combined and dried over $MgSO_4$. Upon filtration, the solvent is removed under reduced pressure to yield a brown oily residue. The photoproducts are isolated by preparative thin layer chromatography (20 × 20 plates; 1000 μm silica gel) with a mobile phase of 60:40 hexanes and ethyl acetate and characterized by ^1H NMR, ^{13}C NMR, and MS (DEI+). The photoproduct obtained was the hydrazine (**9**) and collidine at a 1:1 mol ratio with trace amounts of parent amine (**5**). The hydrazine products have been characterized previously.[49-53] **9b**: ^1H NMR (400 MHz, CD_3CN) δ 7.23 (d, *J* = 8.8 Hz, 8H), 7.02 (d, *J* = 8.8 Hz, 8H). **9c**: ^1H NMR (400 MHz, CD_3CN) δ 7.35 (d, *J* = 9.2 Hz, 8H), 7.15 (d, *J* = 9.2 Hz, 8H); ^{13}C NMR (400 MHz, CD_3CN) δ 142.7, 133.1, 120.1, 115.4; MS (FAB+) *m/z* (rel intensity) 651.7 (6), 571.8 (4), 325.9 (17), 164 (100), 57 (14).

Steady State Analysis. A 3.0 mL portion of the pyridinium salt dissolved in the solvent of choice is taken in a quartz cuvette. The concentration of the reaction mixture is adjusted to have an optical density between 1.5 and 2.0 at 355 nm. Next, 2−3 drops of acid (H_2SO_4 or trifluoroacetic acid) is added to the mixture, which is gently stirred. The sample undergoes photolysis by room light. The UV spectrum is recorded at different time intervals as the photolysis progresses with use of a UV/vis spectrometer. The experiment is conducted in CH_3CN, CH_2Cl_2, $CHCl_3$, chlorobenzene, and nitrobenzene.

Acknowledgment. This work was supported by the Chemistry Division of the National Science Foundation. Arthur Winter assisted with some computational studies. We are also grateful to Prof. Thomas Bally of the University of Fribourg for sharing MOPLOT visualization software.

Supporting Information Available: Detailed synthetic procedures for **1b** and **1c**, ^1H and ^{13}C NMR spectra for compounds **4** and **6**−**9**, miscellaneous LFP spectra, and Cartesian coordinates for optimized singlet and triplet geometries of **2b** and **2c**. This material is available free of charge via the Internet at http://pubs.acs.org.

JO062578I

---

(49) Abakumov, G. A.; Razuvaev, G. A. *Ser. Khim.* **1966**, *10*, 1744.

(50) Cauquis, G.; Delhomme, H.; Serve, D. *Tetrahedron Lett.* **1971**, 4649.

(51) Cauquis, G.; Delhomme, H.; Serve, D. *Electrochim. Acta* **1975**, *20*, 1019.

(52) Neugebau, F. A.; Fischer, H. *Chem. Ber.* **1971**, *104*, 886.

(53) Neugebau, F. A.; Fischer, P. H. H. *Chem. Ber.* **1965**, *98*, 844.